Supplementary information for

Cryo-EM Structure and Oligomerization of the Human Planar Cell Polarity Core Protein Vangl1

Fan Zhang[1,5], Shaobai Li[1,5], Hao Wu[2,3,4,6] and Shanshuang Chen[1,2,3,4,6]

[1]Shanghai Institute of Precision Medicine, Ninth People's Hospital, Shanghai Jiao Tong University School of Medicine, Shanghai, China

[2]Department of Otolaryngology-Head and Neck Surgery, Shanghai Ninth People's Hospital, Shanghai, China

[3]Ear Institute, Shanghai Jiao Tong University School of Medicine, Shanghai, China

[4]Shanghai Key Laboratory of Translational Medicine on Ear and Nose Diseases, Shanghai, China

[5]These authors contributed equally: Fan Zhang, Shaobai Li.

[6]Correspondence to Hao Wu (wuhao@sh9hospital.org) and Shanshuang Chen (chenlab@shsmu.edu.cn)

This supplementary information contains the following content:

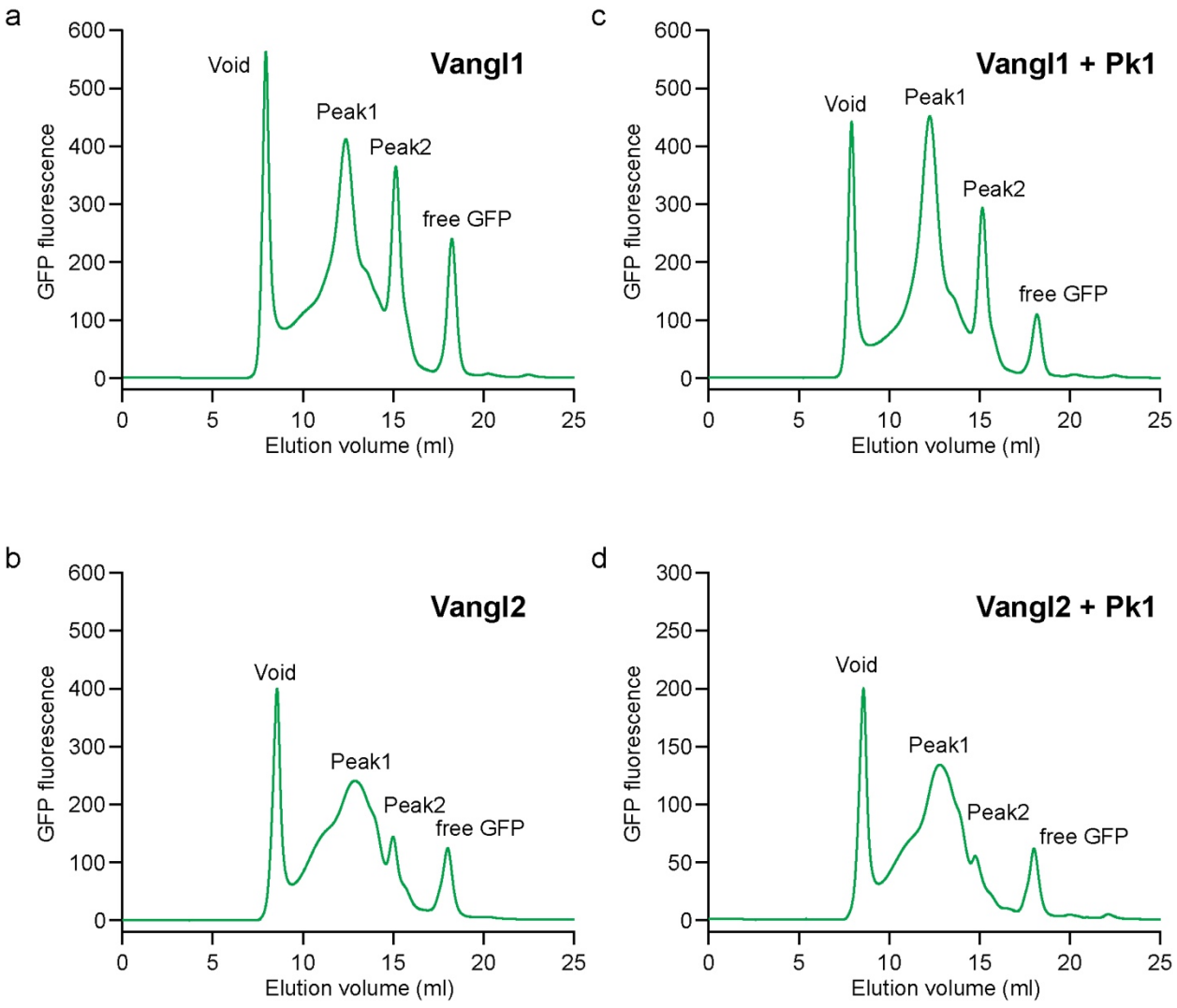

Supplementary Figure 1 | Homogeneity and oligomerization equilibrium of Vangl revealed by FSEC. a-d, FSEC profiles of Vangl1 alone (a), Vangl2 alone (b), Vangl1 co-expressed with Pk1 (c), and Vangl2 co-expressed with Pk1 (d).

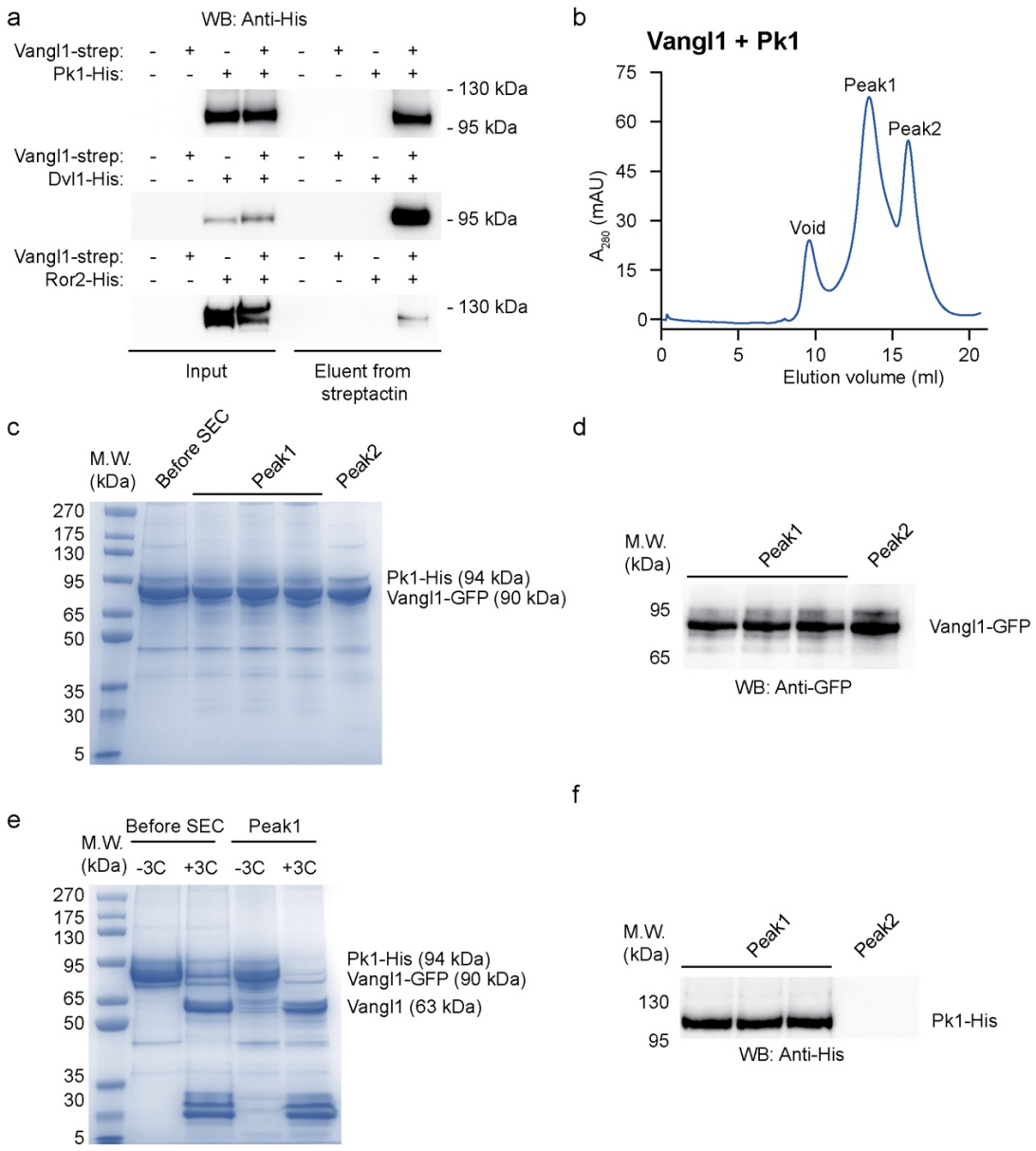

Supplementary Figure 2 | Purification and characterization of Vangl. a, Vangl1 directly interacts with Pk1, Dvl1 and Ror2, as shown by pull down experiments. **b**, Size-exclusion chromatography (SEC) profile of tandem affinity purified Vangl1/Pk1. **c**, SDS-PAGE analysis of the SEC peak fractions from (b). Protein bands were visualized by Coomassie blue staining. **d**, Western blot confirming the presence of Vangl1 in both SEC peaks. **e**, the GFP can be cleaved from Vangl1 by 3C protease revealed by SDS-PAGE analysis. **f**, Western blot showing the presence of Pk1 in Peak 1 but not in Peak 2.

Prickle1 peptide #1
Sequence: ^{635}FSDDVIDNGNYDIEIR^{648}
m/z: 942.93591

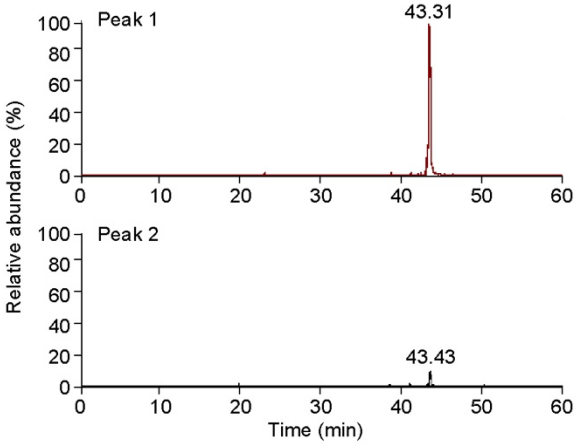

Vangl1 peptide #1
Sequence: ^{311}VYNVDGPSNNATGQSR^{326}
m/z: 839.89282

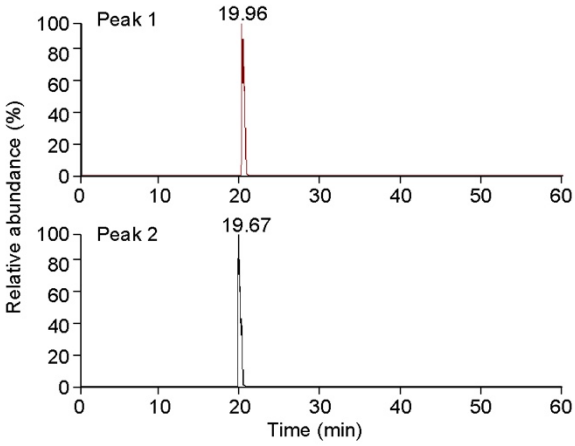

Prickle1 peptide #2
Sequence: ^{348}QSLLLSPALNYK^{359}
m/z: 673.88782

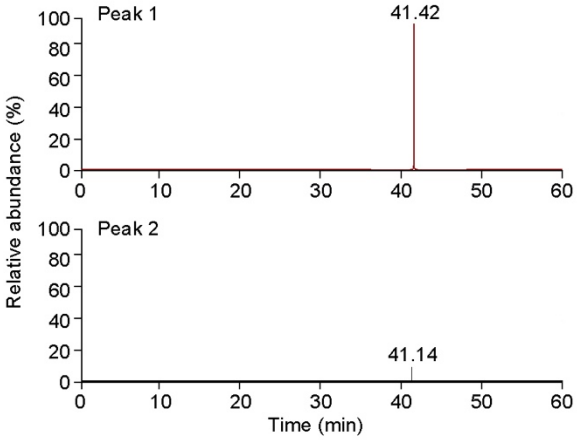

Vangl1 peptide #2
Sequence: ^{465}LVSDEAVTNGLR^{476}
m/z: 637.34253

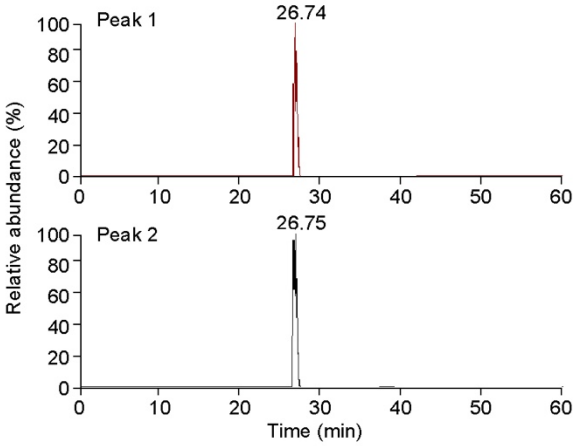

Prickle1 peptide #3
Sequence: ^{305}TCSLGEDVHASDSSDSAFQSAR^{326}
m/z: 1163.99976

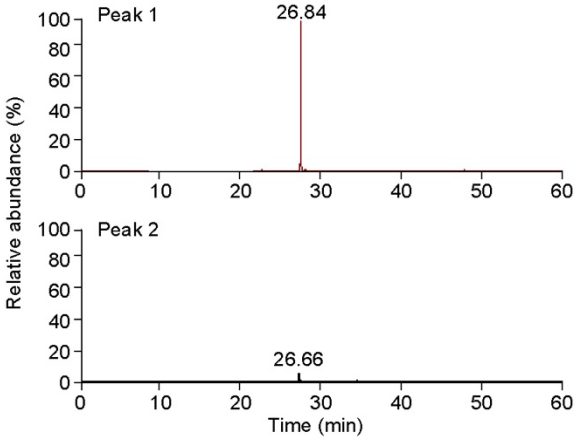

Vangl1 peptide #3
Sequence: ^{477}DGIVFVLK^{484}
m/z: 445.77185

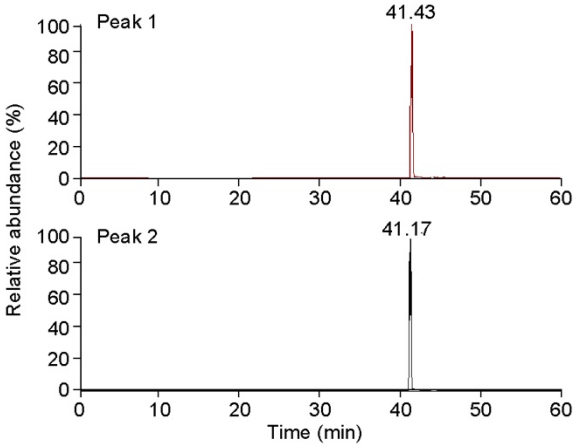

Supplementary Figure 3 | Mass spectrometry analysis of SEC peaks. The relative abundance of Pk1 in Peak 1 and Peak 2 is estimated to be ~10 times different using three independent Pk1 peptides (three panels on the left). In contrast, that of Vangl1 in both peaks is similar (three panels on the right).

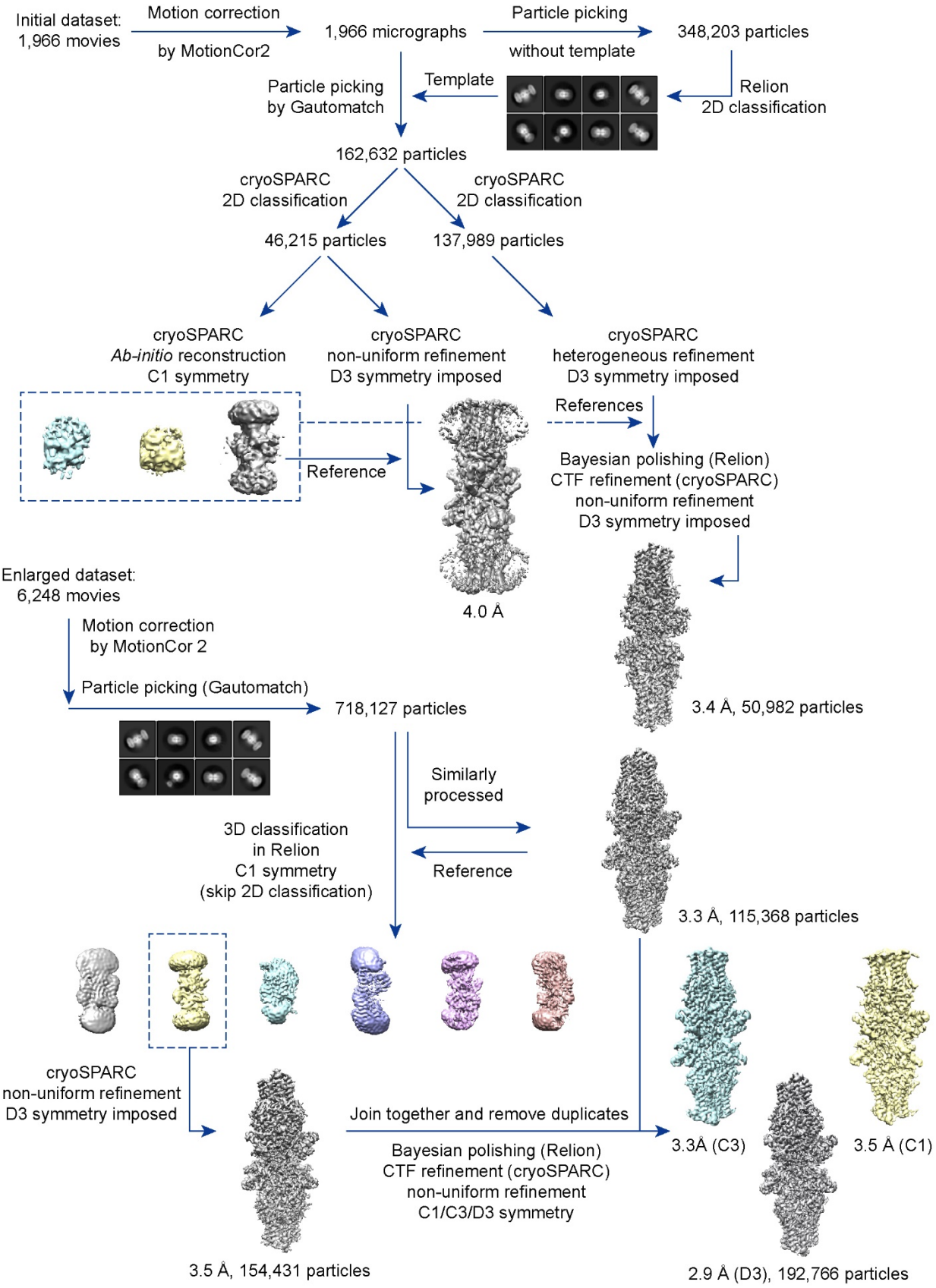
Initial dataset:
1,966 movies
Motion correction
by MotionCor2
1,966 micrographs
Particle picking
without template
348,203 particles
Relion
2D classification
Template
Particle picking
by Gautomatch
162,632 particles
cryoSPARC
2D classification
cryoSPARC
2D classification
46,215 particles
137,989 particles
cryoSPARC
Ab-initio reconstruction
C1 symmetry
cryoSPARC
non-uniform refinement
D3 symmetry imposed
cryoSPARC
heterogeneous refinement
D3 symmetry imposed
References
Reference
Bayesian polishing (Relion)
CTF refinement (cryoSPARC)
non-uniform refinement
D3 symmetry imposed
4.0 Å
Enlarged dataset:
6,248 movies
Motion correction
by MotionCor 2
Particle picking (Gautomatch)
718,127 particles
3.4 Å, 50,982 particles
Similarly
processed
3D classification
in Relion
C1 symmetry
(skip 2D classification)
Reference
3.3 Å, 115,368 particles
cryoSPARC
non-uniform refinement
D3 symmetry imposed
Join together and remove duplicates
Bayesian polishing (Relion)
CTF refinement (cryoSPARC)
non-uniform refinement
C1/C3/D3 symmetry
3.3Å (C3)
3.5 Å (C1)
3.5 Å, 154,431 particles
2.9 Å (D3), 192,766 particles

Supplementary Figure 4 | Workflow of cryo-EM data processing.

Please refer to Methods for details.

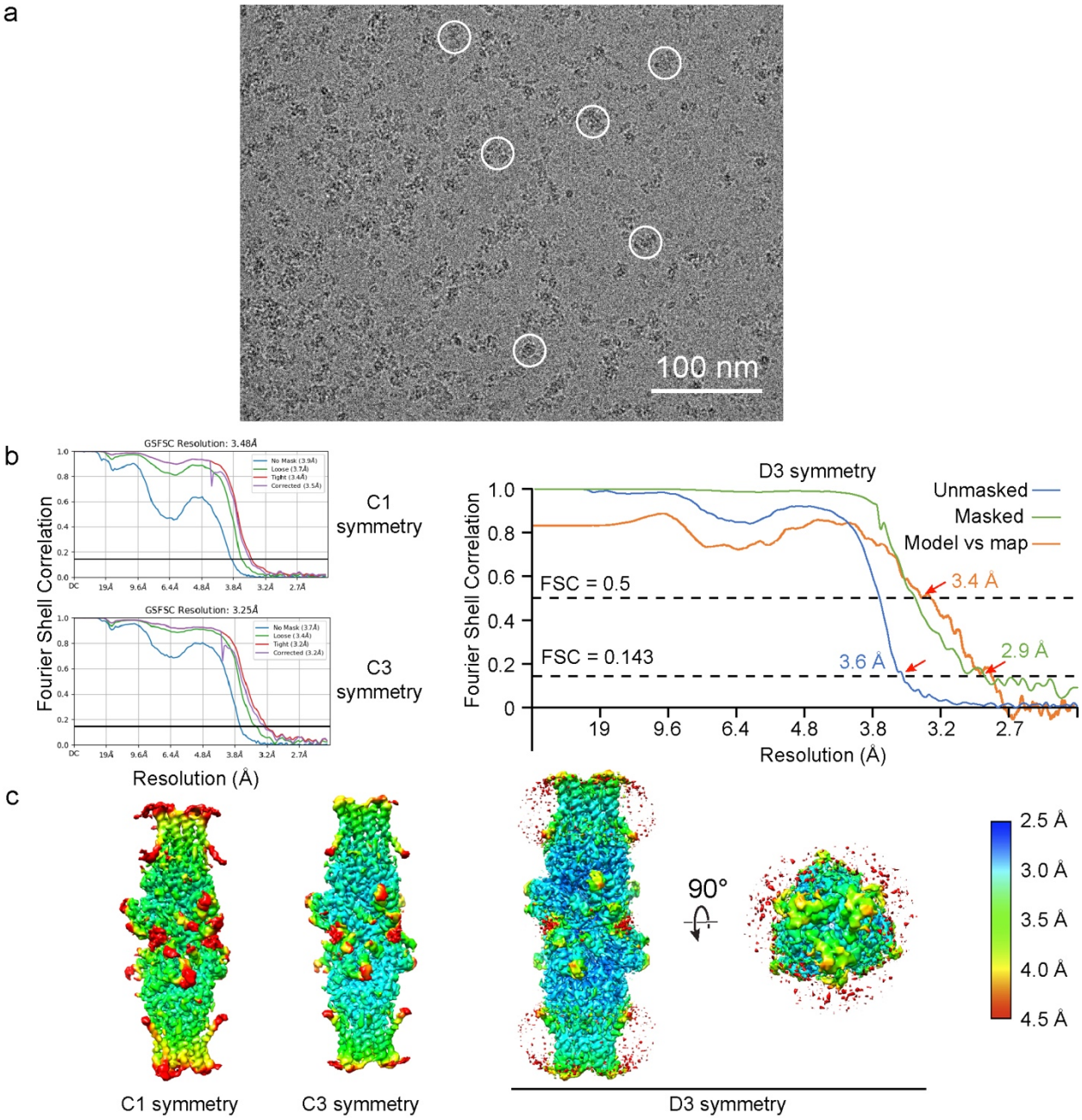
a
100 nm
b
GSFSC Resolution: 3.48Å
GSFSC Resolution: 3.25Å
Fourier Shell Correlation
Resolution (Å)
C1 symmetry
C3 symmetry
D3 symmetry
Unmasked
Masked
Model vs map
FSC = 0.5
FSC = 0.143
3.4 Å
2.9 Å
3.6 Å
c
C1 symmetry
C3 symmetry
90°
D3 symmetry
2.5 Å
3.0 Å
3.5 Å
4.0 Å
4.5 Å
d
Elevation
Azimuth
# of images

Supplementary Figure 5 | Validation of cryo-EM data processing. a, A representative cryo-EM micrograph after motion-correction, with several single particles circled. A scale bar for 100 nm is shown in the corner. **b**, Fourier shell correlation between cryo-EM half maps with or without mask with C1, C3 and D3 symmetry imposed. That between the structural model and the D3-symmetrical cryo-EM reconstruction of D3 symmetry was also plotted. **c**, Local resolution of reconstructions of C1, C3 and D3 symmetry estimated using cryoSPARC. **d**, Angular distribution of the particles used in the final reconstruction.

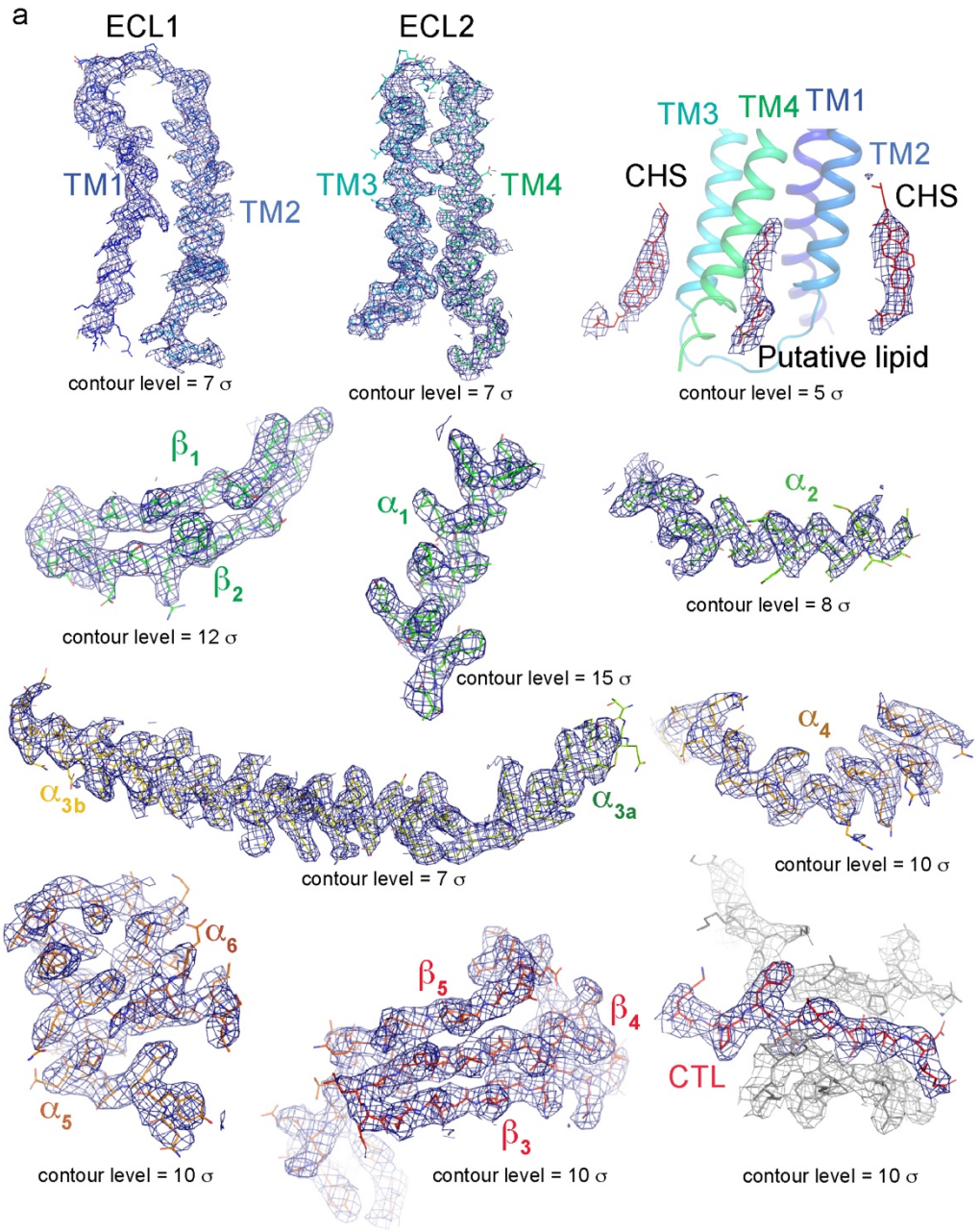
a
ECL1
ECL2
TM1
TM2
TM3
TM4
TM3
TM4
TM1
TM2
CHS
CHS
Putative lipid
contour level = 7 σ
contour level = 7 σ
contour level = 5 σ
β1
β2
α1
α2
contour level = 12 σ
contour level = 15 σ
contour level = 8 σ
α3b
α3a
α4
contour level = 7 σ
contour level = 10 σ
α6
α5
β5
β4
β3
CTL
contour level = 10 σ
contour level = 10 σ
contour level = 10 σ
b
60°
60°

Supplementary Figure 6 | The EM map density of Vangl1. a, Consistent with the 2.9 Å nominal resolution, EM map density for most side chains is clearly visible, thus allowing accurate registry and unambiguous model building. **b**, Three views of the Vangl1 reconstruction without imposed symmetry, 60° apart from each other, where density for Vangl1 were colored in red, cyan and yellow of two different shades, and that putatively for Pk were shown in blue.

Supplementary Figure 7 | Sequence alignment of human Vangl1 and Vangl2. Identical residues are boxed in red, similar residues are represented in red font with white background, variable residues are colored in black. α-helice, β-strands, loops and disordered regions are indicated by cylinders, arrows, solid and dashed lines, respectively, according to the structure.

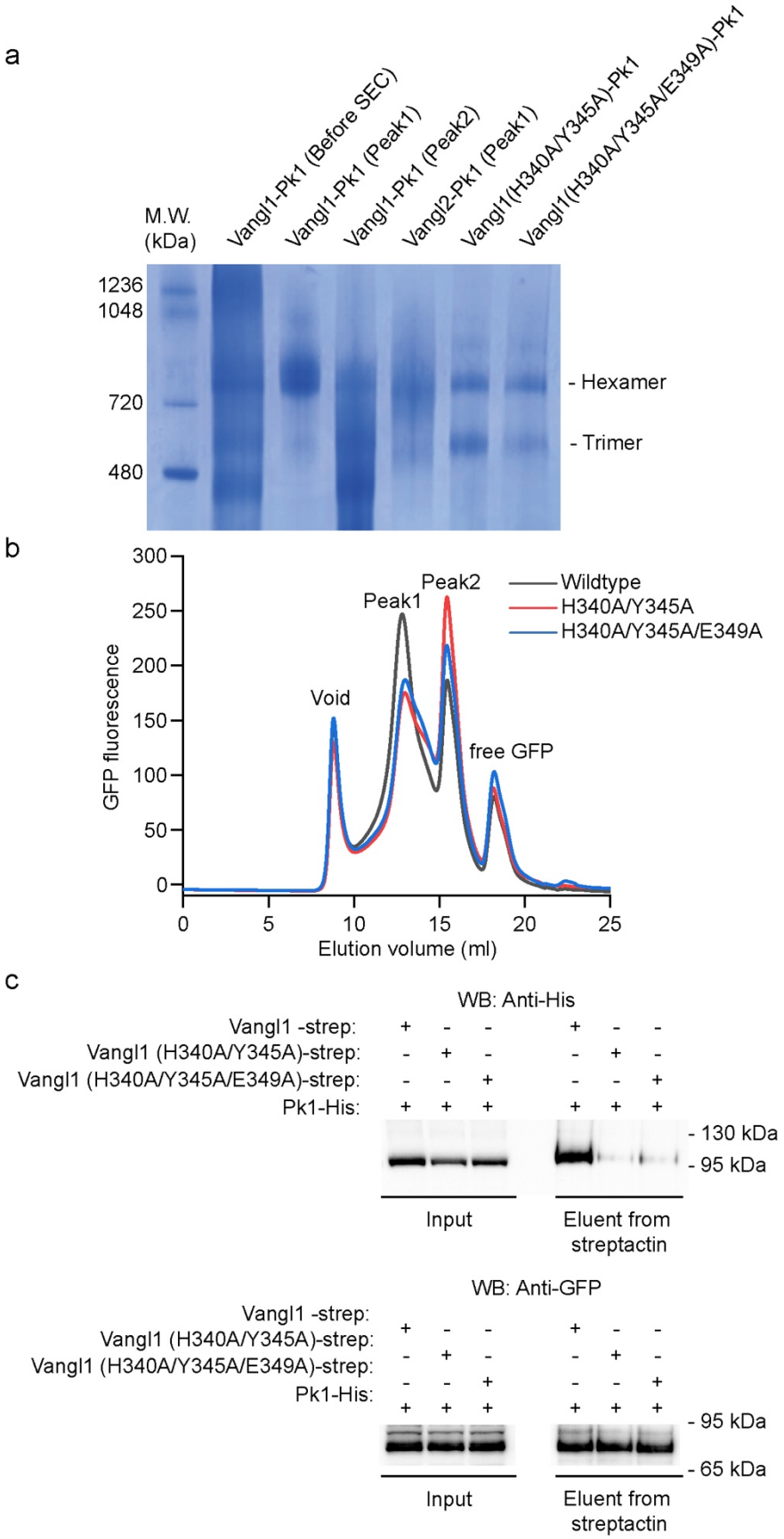
a
M.W. (kDa)
Vangl1-Pk1 (Before SEC)
Vangl1-Pk1 (Peak1)
Vangl1-Pk1 (Peak2)
Vangl2-Pk1 (Peak1)
Vangl1(H340A/Y345A)-Pk1
Vangl1(H340A/Y345A/E349A)-Pk1
1236
1048
720
480
- Hexamer
- Trimer
b
GFP fluorescence
Elution volume (ml)
Void
Peak1
Peak2
free GFP
Wildtype
H340A/Y345A
H340A/Y345A/E349A
c
WB: Anti-His
Vangl1 -strep:
Vangl1 (H340A/Y345A)-strep:
Vangl1 (H340A/Y345A/E349A)-strep:
Pk1-His:
- 130 kDa
- 95 kDa
Input
Eluent from streptactin
WB: Anti-GFP
Vangl1 -strep:
Vangl1 (H340A/Y345A)-strep:
Vangl1 (H340A/Y345A/E349A)-strep:
Pk1-His:
- 95 kDa
- 65 kDa
Input
Eluent from streptactin

Supplementary Figure 8 | Oligomerization equilibrium of Vangl1. a, Blue native PAGE of wild-type Vangl1, Vangl2 and Vangl1 mutants showing the presence of hexmers and trimers. Purification and native PAGE analysis were reproducibly replicated three times. **b**, FSEC profiles of wildtype (WT) Vangl1 in black, Vangl1 with two point mutations (H340A/Y345A) in red and Vangl1 with three point mutations (H340A/Y345A/E349A) in blue, showing mutations introduced at the trimer-trimer interface protomted the presence of trimers. Overexpression and FSEC analysis were reproducibly replicated six times. **c**, The same Vangl1 mutations render compromised ability of pulling down Pk1.

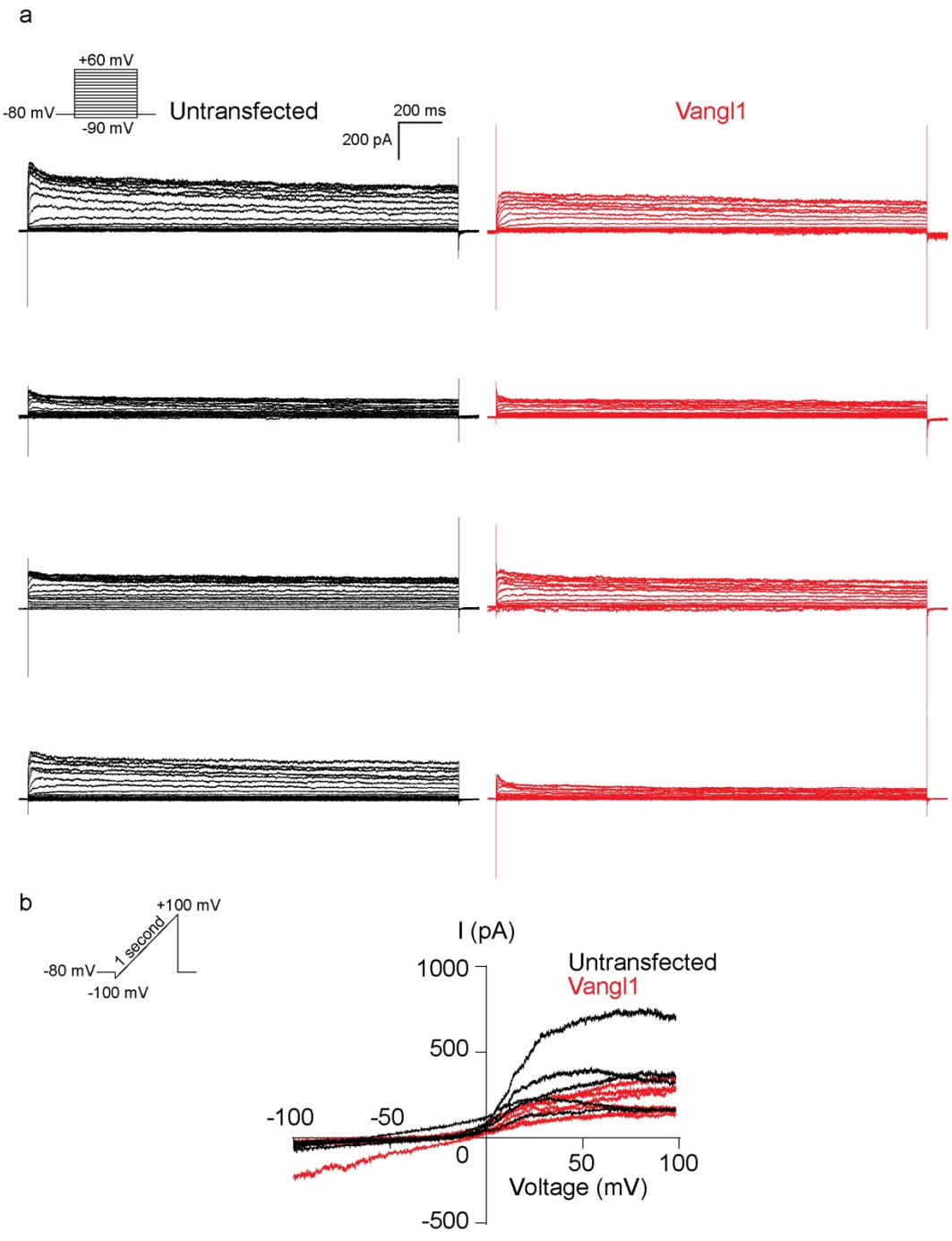

Supplementary Figure 9 | Electrophysiological recordings consistent with the notion that Vangl1 is unlikely to be an ion channel. a-b, Current-voltage relationship was recorded using untransfected HEK293T cells (black) or Vangl1-expressing HEK293T cells (red), which were held at -80 mV before stimulated by a series of voltage steps (a) or a voltage ramp (b).

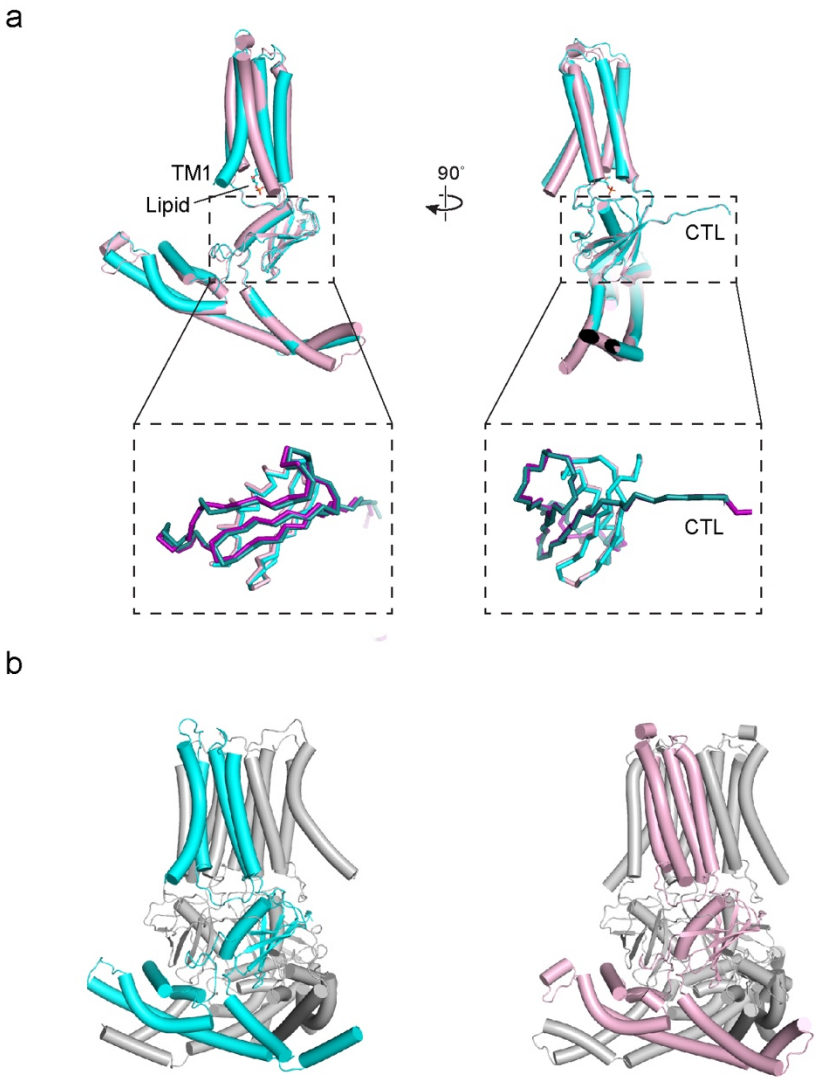

Supplementary Figure 10 | Comparison of the structures of Vangl1 determined by cryo-EM (cyan) and predicted by AlphaFold (light pink). a, Comparison of a protomer revealed consistent overall architecture including the TM domain, the split hand domain, the CTL (inset) and the stick domain, but the kinked TM1 adopts different configuration. **b,** The trimerization of Vangl can be accurately predicted.

Supplementary Table 1 | Statistics of the cryo-EM data collection, refinement and validation.

Statistics for data collection and structural refinement	
	Human Vangl1 PDB 8ZXD EMDB 60540
Data collection and processing	
Microscope	FEI Arctica
Magnification	81000
Voltage (kV)	200
Detector	Falcon 4
Electron exposure ($e^-/Å^2$)	50
Defocus range (μm)	1.5 to 2.5
Pixel size (Å)	1.2
Symmetry imposed	D3
Initial particle images (no.)	718,127
Final particle images (no.)	192,766
Map resolution (Å)	2.9
FSC threshold	0.143
Map resolution range (Å)	2.7-3.9
Refinement	
Initial model used	cryoSPARC *Ab-initio*
Model resolution (Å)	3.4
FSC threshold	0.5
Map sharpening *B* factors ($Å^2$)	-80
Model composition	
Non-hydrogen atoms	19518
Protein residues	2328
B factors ($Å^2$)	
protein	175.03
Ligand	194.48
R.m.s. deviations	
Bond lengths (Å)	0.001
Bond angles (°)	0.403
Validation	
MolProbity score	1.29
Clash score	5.16
Poor rotamers (%)	0
Ramachandran plot	
Favored (%)	97.92
Allowed (%)	2.08
Disallowed (%)	0.00

Supplementary Table 2 | Structural mapping of human disease-associated Vangl mutations.

Diseases/phenotype	Vangl subtype	Mutation Sites (ref.)	Structural location
Neural tube defects	hVangl1	G25K[56]	N-terminal disordered region
	hVangl1	S83L[56]	N-terminal disordered region
	hVangl1	A116T[54]	Transmembrane domain TM1
	hVangl1	F153S[56]	Transmembrane domain TM2
	hVangl1	R173H[57]	Intracellular loop
	hVangl1	R175Q[56]	Intracellular loop
	hVangl1	R181Q[56]	Intracellular loop
	hVangl1	R186H[57]	Transmembrane domain TM3
	hVangl1	A187V[58]	Transmembrane domain TM3
	hVangl1	L202F[56]	Transmembrane domain TM3
	hVangl1	G205R[57]	Transmembrane domain TM3
	hVangl1	R207H[58]	Extracellular Loop 2
	hVangl1	V239I/F[32]	Transmembrane domain TM4
	hVangl1	T251M[56]	Hand domain β_1
	hVangl1	R274Q[32]	Hand domain α_1
	hVangl1	Y290H[56]	Loop region between α_1 and α_2
	hVangl1	M328T[32]	Stick domain α_{3a}
	hVangl1	H350H[58]	Stick domain α_{3b}
	hVangl1	K356K[58]	Stick domain α_{3b}
	hVangl1	R374H[62]	Stick domain α_{3b}
	hVangl1	P384R[80]	Stick domain $\alpha_{3b} - \alpha_4$
	hVangl1	D389H[58]	Stick domain $\alpha_{3b} - \alpha_4$
	hVangl1	A404S[56]	Stick domain α_4
	hVangl1	D468E[56]	Hand domain $\beta_3 - \beta_4$
	hVangl1	R517H[58]	C-terminal disordered region
	hVangl2	S84F[33]	N-terminal disordered region
	hVangl2	R105C[59]	Transmembrane domain TM1
	hVangl2	R135W[59]	Extracellular Loop 1
	hVangl2	R177H[59]	Intracellular loop
	hVangl2	V178I[59]	Intracellular loop
	hVangl2	L242V[59]	Transmembrane domain TM4
	hVangl2	T247M[59]	Hand domain β_1
	hVangl2	R270H[59]	Hand domain α_1
	hVangl2	R353C[33]	Stick domain α_{3b}
	hVangl2	V363E[62]	Stick domain α_{3b}
	hVangl2	F437S[33]	Stick domain α_6
	hVangl2	S464R[62]	Hand domain $\beta_3 - \beta_4$
	hVangl2	R482H[59]	Hand domain β_4
Adolescent idiopathic scoliosis	hVangl1	I136N[55]	Transmembrane domain TM1
	hVangl1	F440V[55]	Stick domain α_6
Sacral agenesis	hVangl1	S338Term[81]	Stick domain $\alpha_{3a} - \alpha_{3b}$
Klippel-Feil syndrome	hVangl1	P384R[80]	Stick domain $\alpha_{3b} - \alpha_4$
Congenital anomalies of the kidney and urinary tract	hVangl2	E70K[82]	N-terminal disordered region
	hVangl2	T433M[82]	Stick domain $\alpha_5 - \alpha_6$
Congenital scoliosis	hVangl1	R256H[60]	Hand domain β_2
	hVangl1	E281G[60]	Hand domain α_2
	hVangl1	R443W[60]	Stick domain α_6
	hVangl2	L226F[60]	Transmembrane domain TM4
Heterotaxy and congenital heart disease	hVangl2	R169H[35]	Intracellular loop
Non-syndromic hearing loss	hVangl2	E465A[35]	Hand domain $\beta_3 - \beta_4$
Congenital heart and brain defects	hVangl2	R135W[35]	Extracellular Loop 1
Looptail	mVangl2	D255E[36]	Hand domain $\beta_1 - \beta_2$
	mVangl2	R259L[83]	Hand domain β_2
	mVangl2	S464N[36]	Hand domain $\beta_3 - \beta_4$
Curly Bob	mVangl2	I268N[61]	Hand domain α_1
NTD-associated mammalian mutations found in *Drosophila* Vang	dVang	D317E[34]	Hand domain $\beta_1 - \beta_2$
	dVang	R321L[34]	Hand domain β_2
	dVang	R332H[34]	Hand domain α_1
	dVang	V391T[34]	Stick domain α_{3a}
	dVang	K418C[34]	Stick domain α_{3b}
	dVang	K577H[34]	C-terminal disordered region

Uncropped images of Western-blots and gels